Interface focus

J. R. Soc. Interface (2010) **7**, S331–S340
doi:10.1098/rsif.2010.0068.focus
Published online 31 March 2010

Biomechanical effects of environmental and engineered particles on human airway smooth muscle cells

P. Berntsen[1,6,†], C. Y. Park[1,†], B. Rothen-Rutishauser[3], A. Tsuda[1], T. M. Sager[1], R. M. Molina[1], T. C. Donaghey[1], A. M. Alencar[4], D. I. Kasahara[1], T. Ericsson[5], E. J. Millet[1], J. Swenson[6], D. J. Tschumperlin[1], J. P. Butler[1,2], J. D. Brain[1], J. J. Fredberg[1,*], P. Gehr[3] and E. H. Zhou[1,*]

[1]*Molecular and Integrative Physiological Sciences, Department of Environmental Health, Harvard School of Public Health, 665 Huntington Avenue, Boston, MA 02115, USA*
[2]*Department of Medicine, Harvard Medical School, 75 Francis Street, Boston, MA 02115, USA*
[3]*Institute of Anatomy, University of Bern, Baltzerstrasse 2, 3000 Bern 9, Switzerland*
[4]*Institute of Physics, University of Sao Paulo, 05508-900 Sao Paulo, Brazil*
[5]*Department of Mathematical Sciences, and* [6]*Department of Applied Physics, Chalmers University of Technology and the University of Gothenburg, 41296 Göteborg, Sweden*

The past decade has seen significant increases in combustion-generated ambient particles, which contain a nanosized fraction (less than 100 nm), and even greater increases have occurred in engineered nanoparticles (NPs) propelled by the booming nanotechnology industry. Although inhalation of these particulates has become a public health concern, human health effects and mechanisms of action for NPs are not well understood. Focusing on the human airway smooth muscle cell, here we show that the cellular mechanical function is altered by particulate exposure in a manner that is dependent upon particle material, size and dose. We used Alamar Blue assay to measure cell viability and optical magnetic twisting cytometry to measure cell stiffness and agonist-induced contractility. The eight particle species fell into four categories, based on their respective effect on cell viability and on mechanical function. Cell viability was impaired and cell contractility was decreased by (i) zinc oxide (40–100 nm and less than 44 μm) and copper(II) oxide (less than 50 nm); cell contractility was decreased by (ii) fluorescent polystyrene spheres (40 nm), increased by (iii) welding fumes and unchanged by (iv) diesel exhaust particles, titanium dioxide (25 nm) and copper(II) oxide (less than 5 μm), although in none of these cases was cell viability impaired. Treatment with hydrogen peroxide up to 500 μM did not alter viability or cell mechanics, suggesting that the particle effects are unlikely to be mediated by particle-generated reactive oxygen species. Our results highlight the susceptibility of cellular mechanical function to particulate exposures and suggest that direct exposure of the airway smooth muscle cells to particulates may initiate or aggravate respiratory diseases.

Keywords: nanoparticles; air pollution; environmental health; mechanobiology; cell mechanics

1. INTRODUCTION

The very large internal surface area of the lungs, approximately 150 m^2 (Gehr *et al.* 1978), is continuously exposed to both innocuous and harmful particulates. These particulates are dealt with by macrophage clearance, the mucociliary escalator and a series of structural and functional barriers (Nicod 2005). Despite the existence of these defences, respiratory diseases are frequent and increasing (Peters *et al.* 1997; Wichmann *et al.* 2000; Schulz *et al.* 2005; Pope *et al.* 2009). Moreover, numerous epidemiological studies have established a causal link between exposure to ambient particulate matter and increased pulmonary and cardiovascular morbidity and mortality (Pope *et al.* 1995; Peters *et al.* 1997, 2001; Lighty *et al.* 2000; Penttinen *et al.* 2001; Dockery *et al.* 2005; Schulz *et al.* 2005; Weichenthal *et al.* 2007).

*Authors for correspondence (jfredber@hsph.harvard.edu; ezhou@hsph.harvard.edu).
†These authors contributed equally to this work.

Electronic supplementary material is available at http://dx.doi.org/10.1098/rsif.2010.0068.focus or via http://rsif.royalsocietypublishing.org.

One contribution to a Theme Supplement 'Mechanobiology'.

Received 9 February 2010
Accepted 8 March 2010

These findings raise the important question of how and over what time scale particulates evade host defences. Consistent with the ability of nanoparticles (NPs), but not micrometre-sized particles (MPs), to penetrate through the submicrometre-thick air–blood barrier (Gehr *et al.* 1978; Geiser *et al.* 2005), recent studies indicate a potential toxic risk of inhaled NPs, mainly combustion-derived particles smaller than 0.1 μm in diameter (Borm & Kreyling 2004; Araujo *et al.* 2008). A new source for airborne NPs is associated with the booming nanotechnology industry and its many related products, especially engineered NPs (Mazzola 2003; Paull *et al.* 2003). Nonetheless, the ability of engineered NPs to cause adverse health effects following accidental or occupational exposure is not well understood (Maynard *et al.* 2006).

The deposition and clearance of particles in the lung are particle-size dependent. Data and computer models suggest that while large (greater than 1 μm) and very small (less than 2 nm) particles tend to deposit in the nasopharyngeal compartment, intermediate-sized NPs (2–100 nm) exhibit significant deposition in the alveolar and tracheobronchial compartments (Oberdorster *et al.* 2005). The deeper the particles are deposited in the lung, the longer it takes to clear them and the higher is the probability of adverse health effects owing to particle–tissue and particle–cell interactions (Rothen-Rutishauser *et al.* 2009). Adverse health effects may also be caused by NPs penetrating into the capillary blood and subsequent translocation into other organs (Kreyling *et al.* 2002; Geiser *et al.* 2005; Muhlfeld *et al.* 2007). There, NPs may alter the organ function through direct interaction with key cell types. *In vitro* studies using cell cultures are providing mechanistic insights into the action of NPs on neurons (Pisanic *et al.* 2007), epithelial cells, macrophages, dendritic cells (Rothen-Rutishauser *et al.* 2005, 2007, 2008) and cardiac muscle cells (Helfenstein *et al.* 2008). Owing to its proximity to the lung epithelium, the airway smooth muscle cell is susceptible to direct exposure to NPs; this indeed has been observed in human biopsy (Pinkerton *et al.* 2000; Churg *et al.* 2003). Nonetheless, the airway smooth muscle cell has received little attention, even though its altered contractile and relaxing responses are intimately related to airway hyper-responsiveness, asthma and other respiratory diseases (Bai 1990; Fredberg *et al.* 1996; Shore 2004; An *et al.* 2006).

In this paper we focus on the human airway smooth muscle (HASM) cell and investigate the effects of eight particle species on the HASM cell's contractile and relaxing responses to biochemical agonists using optical magnetic twisting cytometry (OMTC; Fabry *et al.* 2001*a*; Bursac *et al.* 2005; Deng *et al.* 2006; Trepat *et al.* 2007; Zhou *et al.* 2009). We compared the particulate effect of six different materials: two combustion-derived polydisperse particles included welding fumes (WF) and diesel exhaust particles (DEPs), both of which have significant nanosized fractions (Donaldson *et al.* 2005); engineered NPs included titanium dioxide (TiO_2), fluorescent polystyrene spheres (FS), zinc oxide (ZnO) and copper(II) oxide (CuO). We also assessed the particle-size effect by comparing the ZnO and CuO NPs with their micrometre-sized counterparts. The particles fell into four categories, based on their respective effect on cell viability and on mechanical function. Importantly, we demonstrate that particles could alter cell mechanics dose dependently with little or no concomitant change in cell viability.

2. MATERIAL AND METHODS

2.1. Cell culture and particle/drug treatments

HASM cells were maintained in Ham's Nutrient Mixture F-12 medium supplemented with 10 per cent foetal bovine serum (FBS), 100 U ml^{-1} penicillin, 100 μg ml^{-1} streptomycin, 200 μg ml^{-1} amphotericin B, 12 mM NaOH, 1.6 mM $CaCl_2$, 2 mM L-glutamine and 25 mM HEPES. We plated cells (passages 5–7) in collagen I-coated 96-well plastic plates (Corning, Corning, NY, USA) at 20 000 cells per well and waited 4–6 days before switching the serum-containing media to serum-free media supplemented with insulin (5.7 μg ml^{-1}) and transferrin (5 μg ml^{-1}) (IT media). After 24 h of serum deprivation, we started the treatment with either particles or chemicals, both of which were suspended or dissolved in the IT media. Since we added 0.2 ml media per well, a particle dosage of 1 μg ml^{-1} is equivalent to 0.625 μg cm^{-2}. This treatment lasted for 16–22 h before biomechanical or biochemical measurements. We also tested the effect of hydrogen peroxide (H_2O_2) and zinc chloride ($ZnCl_2$; Sigma-Aldrich), following the same procedure as with particles.

2.2. Preparation of particle suspensions

Eight particle species were used: DEP (SRM 2975 from National Institute of Standards and Technology, USA), WF (0.92–1.38 μm; metal arc welding using mild steel; Antonini *et al.* 1999), TiO_2 (25 nm; Aeroxide from Evonik Degussa Corporation, NJ, USA), FS (40 nm; carboxylate-modified polystyrene FluoSpheres, Invitrogen), $CuO^{5\ \mu m}$ (less than 5 μm; Sigma-Aldrich), $CuO^{50\ nm}$ (less than 50 nm; Sigma-Aldrich), $ZnO^{40\ nm}$ (40–100 nm; Alfa Aesar) and $ZnO^{44\ \mu m}$ (less than 44 μm; Alfa Aesar). Particles were weighed (except for FS, which was suspended in water and pipetted) and suspended directly in the IT media at 10 mg ml^{-1}. The suspensions were sonicated for 20–30 s using a sonicator (Sonifier Cell Disruptor, model no. W200P, Heat systems-ultrasonics Inc., Plainview) right before adding to cells. We always prepared fresh particle suspensions right before the treatment.

2.3. Optical magnetic twisting cytometry assay

OMTC is a high-throughput tool for quantifying adherent cell mechanics with remarkable temporal and spatial resolution (Fabry *et al.* 2001*b*). Briefly, we produced 4.5 μm ferromagnetic beads and coated them with poly-L-lysine (PLL; 4 kDa) at 75 μg PLL per mg beads. This coating allows avid binding to cell surface and has been shown to give similar cell stiffness measurements compared with coating with RGD peptides (Bursac *et al.* 2007; Zhou *et al.* 2009). However, PLL does not induce integrin clustering and focal

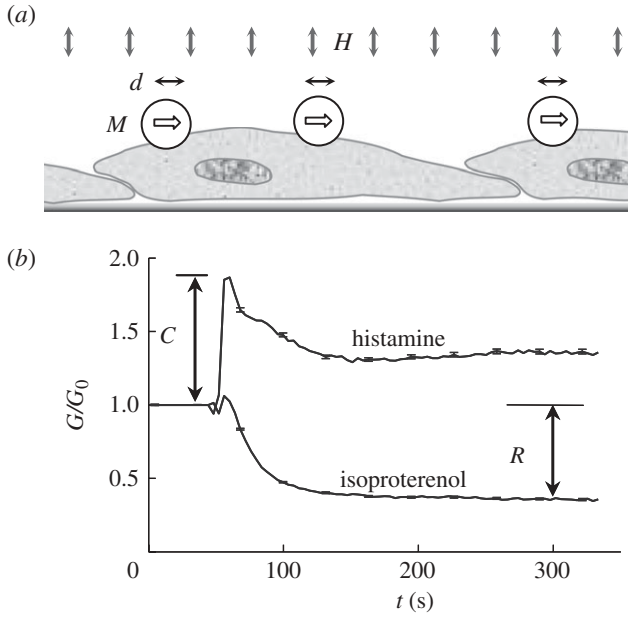

Figure 1. The measurement of cell stiffness, contractile response and relaxing response using OMTC. (*a*) The working mechanism of OMTC. The magnetized bead (M) is twisted by the vertical magnetic field (H); the lateral motion of the bead (d) is inversely related to the cell stiffness (G). (*b*) Normalized stiffness changes in response to histamine and isoproterenol are shown for over 1000 untreated cells (median ± s.e.). The maximum contractile response (at approx. 10 s after adding histamine) and maximum relaxing response (at approx. 250 s after adding histamine) are denoted C and R, respectively.

adhesion formation, as RGD does; therefore, the passive binding of PLL will cause less alteration in the cell to be measured. PLL offers the additional advantages of better storage stability and dispersion of the coated beads. After overnight particle suspension treatment, we replaced cell media with fresh IT media, thus removing any suspended or loosely bound particles. After 20 min, the coated beads were added and allowed to incubate with the cells for 20–40 min before OMTC measurements; this variability in bead incubation time had little effect on the measured cell stiffness. To measure cell stiffness, the beads were first magnetized horizontally by a large magnetic field; each bead became a small magnet (M). A much weaker magnetic field oscillating at 0.77 Hz (H) was then applied vertically, which applied a sinusoidal torque to the beads. Motion of the beads (d) was optically recorded (figure 1*a*). The ratio between the torque and bead motion thus defined an apparent stiffness for a cell, which had the unit Pa nm^{-1}. In a typical run, we would start the twisting field to continuously monitor cell stiffness for a few hundred cells, add histamine (100 μM) or isoproterenol (100 μM), both from Sigma-Aldrich, at 50 s and continue twisting for another 5 min. This would allow us to obtain three quantities, the stiffness prior to applying agonist (G_0), the maximum response to isoproterenol (R) and the maximum response to histamine (C); the latter two are illustrated in figure 1*b*. All measurements were performed at 37°C. Custom software was written in MATLAB to automate the large-volume data analysis.

2.4. Alamar Blue assay

We determined cell viability using Alamar Blue (Invitrogen). Cells were cultured and treated with particles using the same procedure as for OMTC assay, with the same number of cells per well. Alamar Blue was added to each well at 10 per cent volume and incubated for 200 min. Metabolically active cells reduce the dye into a fluorescent form, and this fluorescent emission signal was measured using a plate reader (excitation/emission: 544 nm/590 nm; Fluoroskan Ascent Plate Reader, ThermoFisher). The emission signal was used to estimate cell viability by linear interpolation between the emission from cells treated with 0.1 per cent saponin (0% viability) and that from untreated cells (100% viability). We compensated for the possible interference of particles with the Alamar Blue assay using the procedure below.

To test whether the presence of particles interferes with this fluorescence-based assay, we performed a cell-free experiment. We first incubated IT media containing 10 per cent Alamar Blue with fully confluent, untreated HASM cells in culture flasks for 200 min; the fully reduced media then represent 100 per cent viability. These media were collected and particles added to them at the same doses as in cell treatments. We loaded the particle suspensions, together with positive control (fully reduced media with no particle) and negative control (IT with 10% fresh Alamar Blue), in a 96-well plate, incubated overnight in a cell culture incubator and read the fluorescence the next day. This incubation mimics the procedure for cell treatment, during which the particles partially sediment. Using linear interpolation between negative control and positive control, we can estimate a nominal viability. Since our cell-free assay defined the emission signal for 100 per cent viability for all particles at all doses, we can use this nominal viability to compensate for any artefact introduced by the presence of the particles, by normalization.

2.5. Statistical analysis

For the OMTC assay, statistical comparisons with no-particle control were made using the Kruskal–Wallis non-parametric one-way analysis of variance by ranks. For the cell viability assay, statistical comparisons with no-particle control were made using Student's *t*-test with two tails and unequal variance. A difference was considered significant if $p \leq 0.01$. We list all the sample sizes in the electronic supplementary material, table S1, for OMTC assay and in the electronic supplementary material, table S2, for the Alamar Blue assay; each experiment was repeated at least once on a different day. For OMTC assay, we report the median with standard errors; for cell viability indices, we report the mean with standard errors. We note that the error bars are often so small that they are masked by the data symbol.

3. RESULTS

The results are presented first with respect to viability over all particulate species. This is followed by the results for cell mechanics. We conclude this section by exploring the role of reactive oxygen species (ROS).

3.1. Effects of particles on viability

In contrast to the claim that the Alamar Blue assay is not affected by particulates (Fahmy & Cormier 2009), our cell-free experiment demonstrated that some particles can interfere with this assay. FS (polystyrene NPs) and TiO_2 dose dependently increased the nominal viability by up to 20 per cent at 200 $\mu g\,ml^{-1}$; whereas $CuO^{50\,nm}$ and DEPs dose dependently decreased the nominal viability by up to 19 and 16 per cent, respectively, at 200 $\mu g\,ml^{-1}$ (electronic supplementary material, figure S1, left). The other particles did not interfere with the Alamar Blue assay. The raw Alamar Blue data for particle-treated cells are shown in the electronic supplementary material, figure S1, right, in which FS and TiO_2 artificially caused a dose dependent increase in viability beyond 100 per cent. To compensate for the artefacts introduced by the presence of the particles, we normalized the raw Alamar Blue viability with the nominal viability that we measured in the absence of cells with the same particle species and dose.

Up to 200 $\mu g\,ml^{-1}$, TiO_2, DEP, FS and WF did not decrease cell viability by more than 20 per cent (figure 2*a*). While consistent with independent findings on TiO_2 and DEP (Lehmann *et al.* 2009; Müller *et al.* 2009), these findings differed from those of others on FS toxicity on rat lung macrophages (Frohlich *et al.* 2009) and on WF toxicity on a human endothelial cell line (Antonini *et al.* 1999). Better controlled experiments are needed to determine whether HASM cells are more tolerant of these two particles than those other cell types.

ZnO was remarkably toxic for HASM cells, with significant but relatively small dependence on particle size (figure 2*c*). With nearly 1000-fold difference in size, the 50 per cent lethal dose (LD50) for $ZnO^{44\,\mu m}$ is only 49 per cent higher than that for $ZnO^{40\,nm}$ (table 1), presumably owing to a slower dissolution rate for the former. Furthermore, $ZnO^{40\,nm}$ exhibited toxicity

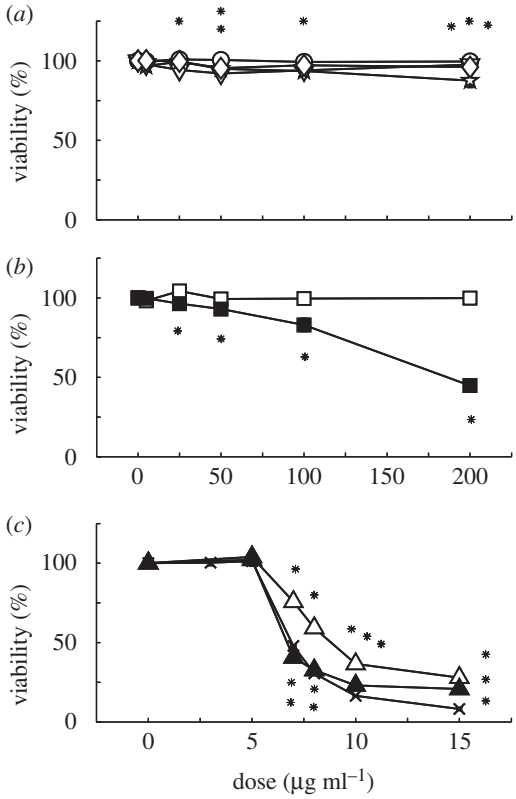

Figure 2. The effect of eight particles on the viability of HASM cells after correcting for the optical interference of particles. (*a*) At the doses tested, TiO_2, DEP, FS and WF caused little change in cell viability. (*b*) CuO NPs, but not MPs, caused dose-dependent decrease in viability. (*a*) and (*b*) have the same *x*-axis. (*c*) Both ZnO NPs and MPs impaired cell viability, with the former being more toxic. Also shown here is the soluble $ZnCl_2$. In this and all subsequent figures, an asterisk indicates statistically significant difference from the negative control ($p < 0.01$). (*a*) Lines with open circles, TiO_2; lines with open inverted triangles, DEP; lines with stars, FS; lines with open diamonds, WF. (*b*) Lines with open squares, $CuO^{5\,\mu m}$; lines with filled squares, $CuO^{50\,nm}$. (*c*) Lines with open triangles, $ZnO^{44\,\mu m}$; lines with filled triangles, $ZnO^{40\,nm}$; lines with crosses, $ZnCl_2$ (the actual mass dose was scaled by MW_{ZnO}/MW_{ZnCl_2} to match the zinc concentration; MW, molecular weight).

similar to that of soluble $ZnCl_2$ at the same zinc concentration (figure 2*c*). This suggests that the toxicity for these particles is largely a consequence of soluble Zn^{2+}, consistent with the considerable solubility of ZnO (Xia *et al.* 2008). Thus, while essential for a wide range of biochemical reactions, excess zinc can impair cell physiology (Dineley *et al.* 2003; Sharpley & Hirst 2006; Gazaryan *et al.* 2007).

Interestingly, CuO particles exhibited size-dependent toxicity. CuO NPs decreased cell viability dose dependently with an LD50 of 186.4 $\mu g\,ml^{-1}$; by contrast, the MPs did not alter cell viability (figure 2*a* and table 1). This finding is consistent with a previous report (Karlsson *et al.* 2009).

3.2. Effects of particles on cell mechanics

Having determined toxicity of the various particles as a function of species and size, we quantified the changes

Table 1. LD50 and ED50 values for the effect of particulates on HASM cell viability, stiffness, contraction to histamine and relaxation to isoproterenol. Doses have the unit of $\mu g\ ml^{-1}$ ($1\ \mu g\ ml^{-1} \sim 0.625\ \mu g\ cm^{-2}$).

			ED50		
	size	LD50	stiffness	contraction	relaxation
TiO_2	25 nm	>200	>200	>200	>200
DEP	polydisperse	>200	>200	>200	>200
FS	40 nm	>200	21.8	26.9	17.4
WF	0.92–1.38 μm	>200	[a]	>200	>200
$CuO^{5\ \mu m}$	<5 μm	>200	>200	>200	>200
$CuO^{50\ nm}$	<50 nm	186.4	25.9	34.6	27.8
$ZnO^{44\ \mu m}$	<44 μm	8.8	7.9	6.9	6.9
$ZnO^{40\ nm}$	40–100 nm	6.7	6.4	5.6	5.9

[a]Not inhibited, but rather increased by over 100% at $50\ \mu g\ ml^{-1}$ (see figure 6).

in the mechanical functions of the HASM cell following particulate exposure. For these functional assays, we employed much lower concentrations where the viability is decreased by no more than 10 per cent, except for ZnO particles. Up to $50\ \mu g\ ml^{-1}$, TiO_2 and DEP altered the cell stiffness, contraction induced by histamine and relaxation induced by isoproterenol by no more than 50 per cent; these alterations exhibited no clear dose dependence (figure 3). The moderate effect of TiO_2 and DEP we observed here is consistent with their moderate effects on cardiomyocyte electrophysiology (Helfenstein *et al.* 2008).

Exposure to ZnO elicited a different response. At doses below $5\ \mu g\ ml^{-1}$, the intrinsic stiffness and isoproterenol response changed little, while histamine response increased moderately (figure 4*a–c*). However, at $7\ \mu g\ ml^{-1}$, all three indices nearly vanished for $ZnO^{40\ nm}$; the same occurred for $ZnO^{44\ \mu m}$-treated cells at $10\ \mu g\ ml^{-1}$ (figure 4*a–c*). Consistent with cell viability assay, the OMTC assay suggested that the ZnO NPs are moderately more effective at impairing the biomechanical function than the MPs. To quantitatively compare the viability assay and the biomechanical assay, we looked at the effective doses for 50 per cent inhibition (ED50) and LD50 (table 1). For each ZnO particle, the ED50 and LD50 are quite comparable. This suggests that a cytotoxicity mechanism accounts for both the loss of viability and the impairment of cell mechanics, presumably through depletion of ATP (Dineley *et al.* 2003).

Despite the fact that Cu^{2+} and Zn^{2+} ions are both divalent, the CuO particles differ fundamentally from ZnO in their effects on HASM cells. CuO MPs are much less toxic than CuO NPs, as shown above. Our OMTC assay further revealed little change in the cell stiffness (figure 5*a*), contraction (figure 5*b*) or relaxation (figure 5*c*) with the cells exposed to up to $50\ \mu g\ ml^{-1}$ MPs. By contrast, the NPs caused a dramatic dose-dependent decrease in all three indices, with nearly 100 per cent inhibition at $50\ \mu g\ ml^{-1}$ (figure 5). At this dose, the Alamar Blue assay revealed only 7 per cent decrease in viability; consistently, LD50 was five times higher than ED50 (table 1). Thus, unlike ZnO, CuO NPs could inhibit cell stiffness and contractility with minimal impairment of viability.

Exposure of particles to other species also showed that cell mechanics could be altered without affecting viability. FS particles of 40 nm induced a dose-dependent inhibition of stiffness, contraction and relaxation of the HASM cells (figure 6). By contrast, while it did not affect cell stiffness or relaxation, WF greatly enhanced cell contraction in response to histamine (figure 6). These data suggest direct particulate exposure can markedly alter the mechanical properties and function of the HASM cell.

3.3. The role of reactive oxygen species

What are the mechanisms of action responsible for the diverse changes in cellular viability and mechanics? While detailed biochemical analysis is beyond the scope of the current work, we addressed the potential role of ROS in mediating these changes. ROS are known to be induced by a wide range of particulates and are therefore a candidate pathway leading to NP toxicity (Xia *et al.* 2006). We subjected the HASM cells to ROS by exposure to H_2O_2. Surprisingly, with doses up to 500 μM, H_2O_2 caused no change in viability and did not alter the HASM cell stiffness, contraction or relaxation (electronic supplementary material, figure S2). To rule out the possibility that the H_2O_2 dosage was inaccurate owing to storage, we repeated the cell viability assay using newly purchased H_2O_2 solution and obtained identical results: LD50 for H_2O_2 was 1116 μM (electronic supplementary material, figure S2*d*). Our finding of the high tolerance of HASM cells to H_2O_2 is consistent with a prior report on foetal HASM cells (Pandya *et al.* 2002). Thus, the HASM cells may be more tolerant to H_2O_2 than many other cell types including human fibroblasts (Miyoshi *et al.* 2006) and rat aortic vascular smooth muscle cells (Li *et al.* 2000), which undergo cell death at below 100 μM of H_2O_2. The ROS generated by 500 μM H_2O_2 greatly exceeds that generated by NPs at the doses used here (Xia *et al.* 2008; Frohlich *et al.* 2009). While it does not rule out a role for ROS generation, this observation suggests that the diverse particulate effects on viability and cell mechanics are unlikely to be mediated by generation of ROS.

4. DISCUSSION

In this study, we used the airway smooth muscle cell as a model to investigate the effects of eight particle

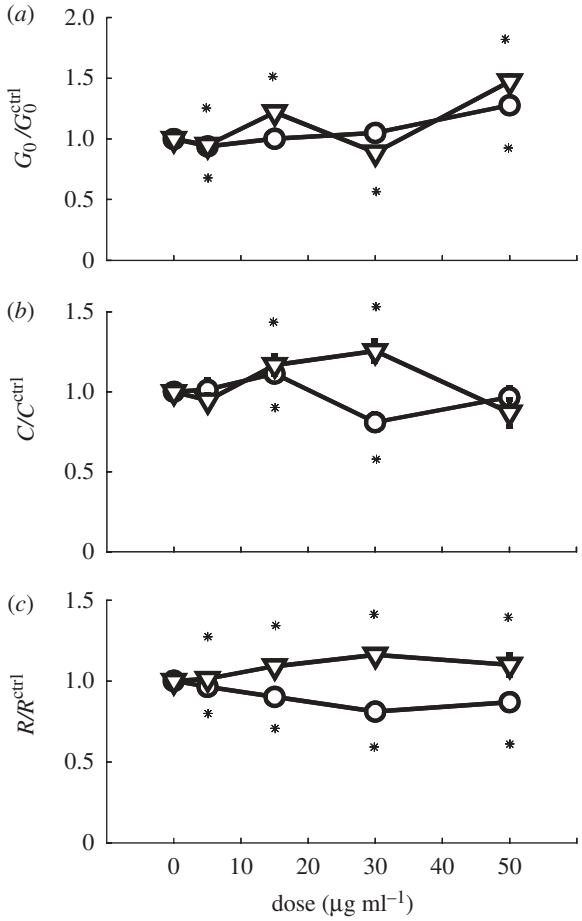

Figure 3. TiO_2 and DEP caused minor changes in (*a*) cell stiffness, (*b*) contractile response induced by histamine and (*c*) relaxing response induced by isoproterenol. All indices have been normalized to those of untreated cells. Lines with open circles, TiO_2; lines with open inverted triangles, DEP.

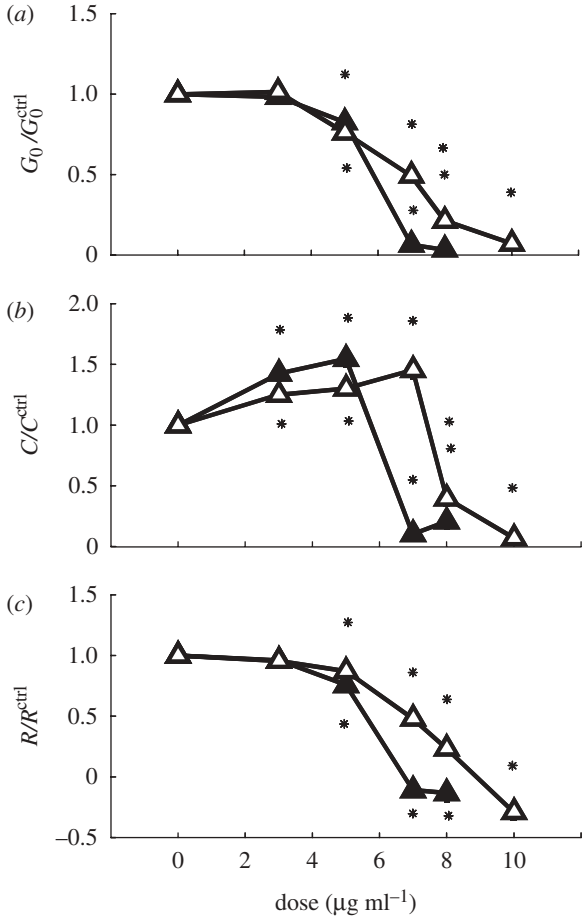

Figure 4. ZnO NPs and MPs caused dose-dependent inhibition of (*a*) cell stiffness, (*b*) contractile response and (*c*) relaxing response. Lines with open triangles, $ZnO^{44\ \mu m}$; lines with filled triangles, $ZnO^{40\ nm}$.

species on cell viability and mechanics. The particles fell into four categories, based on their respective effect on viability and on mechanics (table 2). In support of the enhanced sensitivity of our biomechanics assay, we demonstrated that particles could dose dependently alter cell mechanics with little or no concomitant change in cell viability. In this section, we first discuss particle-size effects. This is followed by a discussion of the mechanism underlying the action of NPs, focusing on NP–macromolecule interaction. We close the discussion by envisioning further applications of biomechanics as a key cellular response and associated pathobiological implications of NP exposure.

4.1. Particle-size effects

A key characteristic of NPs is their significantly increased surface area relative to the same mass of MPs (Oberdorster *et al.* 2005; Nel *et al.* 2006). Particle surface area is proportional to the square of particle diameter, whereas the particle mass is proportional to the cube of particle diameter. It follows that for a given mass, particle surface area is inversely proportional to particle diameter. Enhanced particle surface area with reduced particle diameter can promote direct contact between the constituent atoms or molecules with the macromolecules of the cell; alternatively, that can accelerate dissolution of the particles.

For materials that are largely insoluble, comparisons between NPs and microparticles suggest that the biological responses can be unified if the particle dose was expressed in surface area per unit volume (Sager *et al.* 2008; Sager & Castranova 2009; Waters *et al.* 2009). For CuO particles, their toxicity may not be attributable to the Cu^{2+} ions because copper chelators desferoxamine and D-penicillamine did not reduce the particle toxicity (Fahmy & Cormier 2009). Thus, CuO toxicity is mainly through direct contact between the particle surface and the cell. Indeed, we observed greatly enhanced toxicity of the CuO NPs compared with that of the CuO MPs at a given mass dose, the former having approximately 100 times the surface area of the latter. Our observation of this enhanced toxicity for the CuO NPs is consistent with the findings of others (Fahmy & Cormier 2009; Karlsson *et al.* 2009).

While CuO is largely insoluble, ZnO is quite soluble (Xia *et al.* 2008). Previous studies on eukaryotes have found little difference between ZnO NPs of different sizes (Deng *et al.* 2009; Lin *et al.* 2009). Consistent with this, here we found only a moderate difference in cytotoxicity between ZnO NPs and ZnO MPs. This difference probably results from a difference in dissolution rate, with the NPs dissolving faster than the

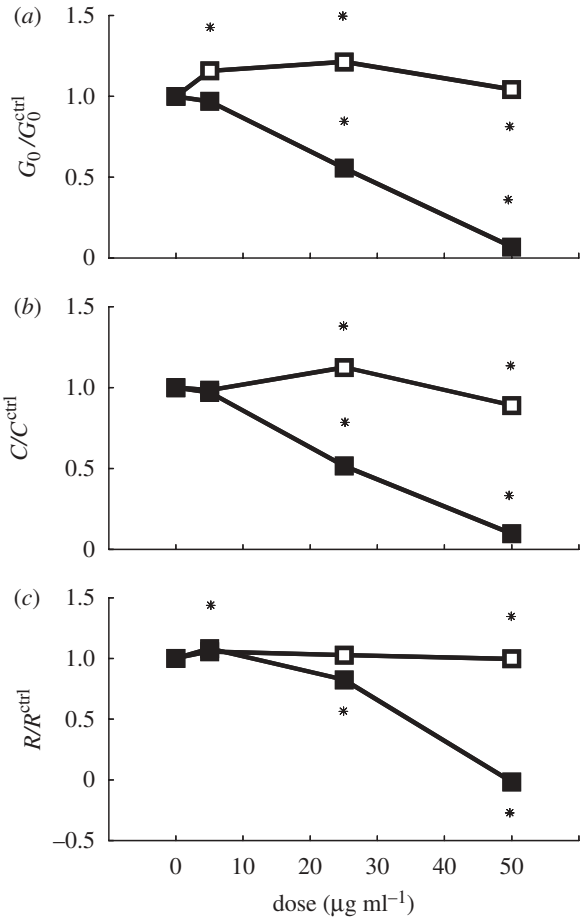

Figure 5. CuO NPs, but not MPs, caused dose-dependent inhibition of (*a*) cell stiffness, (*b*) contractile response and (*c*) relaxing response. Lines with open squares, $CuO^{5\ \mu m}$; lines with filled squares, $CuO^{50\ nm}$.

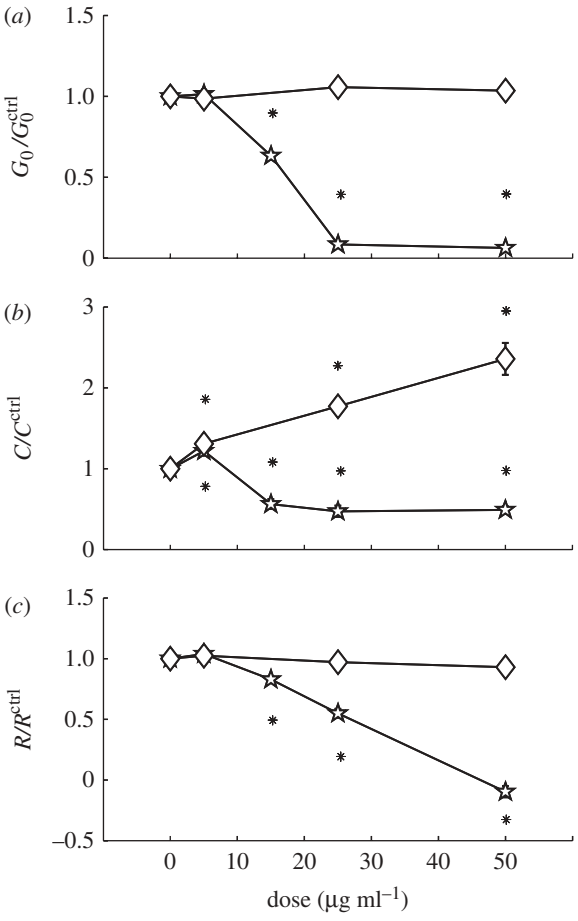

Figure 6. FS and WF changed cell mechanics in opposite ways. FS dose dependently inhibited (*a*) stiffness, (*b*) contraction and (*c*) relaxation. By contrast, WF had little effect on (*a*) stiffness or (*c*) relaxation, but (*b*) dose dependently enhanced contractile response to histamine. Lines with stars, FS; lines with diamonds, WF.

MPs. Nonetheless, for a difference of 1000-fold in particle size, the difference in LD50 was only 49 per cent. Thus, while the efficacy of insoluble particles is largely determined by their surface area, the efficacy of soluble particles is mainly determined by their mass.

4.2. Reactive oxygen species generation or nanoparticle–macromolecule interaction

The cytotoxic and physiological effects of NPs are currently unclear. Copper chelators did not inhibit the cytotoxicity of CuO NPs, suggesting that the toxicity is associated with the CuO particles (Fahmy & Cormier 2009). Those authors further demonstrated that CuO NPs generated a moderate amount of ROS, yet there was much oxidation of glutathione and production of 8-isoprostane, both pointing to increased oxidative stress; the cytotoxicity and production of 8-isoprostane could be partially inhibited by resveratrol, an antioxidant (Fahmy & Cormier 2009). We observed similar cytotoxicity of the CuO NPs on HASM cells. However, the cells were resistant to the application of high concentration of ROS (H_2O_2), suggesting a relatively high capacity of the native antioxidant machinery. We suggest that the induction of oxidative stress without much production of ROS by the CuO NPs (Fahmy & Cormier 2009) is more likely owing to a direct inhibition of the antioxidant macromolecules by the particles. Furthermore, certain NPs are cytotoxic in the absence of oxidative stress (Frohlich *et al.* 2009). We cannot rule out ROS generation and oxidative stress as consequences of cell–NP interaction, but they might be downstream of NP–macromolecule interaction, as we further argue below.

Table 2. Categorization of particles by their respective effect on cell viability and on cell mechanics.

	LD50 <200 μg ml^{-1}	LD50 >200 μg ml^{-1}
decreased contractility	$ZnO^{7\ nm}$, $ZnO^{40\ nm}$, $CuO^{50\ nm}$	$FS^{40\ nm}$
increased contractility		WF
little change		DEP, $TiO_2^{25\ nm}$, $CuO^{5\ \mu m}$

Data from others and the current study suggest that ZnO toxicity is mainly a consequence of soluble Zn^{2+}. The specific mechanism of zinc toxicity is still unclear, but it is known that at least 10 per cent of the proteome

has Zn^{2+} binding domains (Li & Maret 2009; Maret & Li 2009). The free intracellular Zn^{2+} is normally extremely low and tightly regulated. Thus, dissociated Zn^{2+} from ZnO particles can overwhelm the buffering capacity of key proteins such as the metallothioneins (Henkel & Krebs 2004; Li & Maret 2008). The excessive free Zn^{2+} can bind to and change conformations of a wide range of proteins, and this can lead to massive dysregulation of the signalling pathways, ultimately causing cell death. Thus, we suggest that probing both specific and non-specific interactions between NPs and macromolecules is vital to understanding the diverse biological effects of NPs (Klein 2007).

4.3. Cell biomechanics and particle research

Diverse macromolecules in cells assemble into filaments and form the cytoskeleton. It is the cytoskeleton that confers stiffness and contractility to the cell (Elson 1988; Zhu *et al.* 2000; Lim *et al.* 2006*b*). Measuring these properties can therefore serve as a sensitive tool for probing the organization of the cytoskeleton (Lim *et al.* 2006*a*; Suresh 2007; Zhou *et al.* in press), and also the signalling pathways that control the cytoskeleton. NPs may alter cytoskeletal organization and processes through direct or indirect mechanisms. While most NPs enter the cell via caveolin- and clathrin-mediated endocytosis, a subset of NPs enter the cell by adhesive interactions and are found free in the cytoplasm (Geiser *et al.* 2005; Rothen-Rutishauser *et al.* 2009). This subset of NPs thus have the potential to directly interact with the cytoskeleton and the contractile machineries. Alternatively, particles can inhibit, cluster or even signal to cell-surface receptors, and thus result in downstream changes in cytoskeletal structure (as probed using cell stiffness) and altered receptor signal transduction (as probed using histamine/isoproterenol responses, both targeting cell-surface receptors). Indeed, our biomechanical assays revealed sensitive alterations in the stiffness and pharmacological responses when the HASM cells are exposed to a few specific particulates.

Our findings demonstrating alterations in cytoskeleton mechanics relate to a few prior reports and can shed light on the action of NPs. Inhalation exposure of rats to gold NPs resulted in significant downregulation of many muscle genes, such as myosin, troponin and tropomyosin, in the lung (Yu *et al.* 2007). Thus, the inhaled gold NPs may have induced changes in the pulmonary vessel smooth muscle and/or the respiratory smooth muscle. It remains to be investigated whether this downregulation in muscle genes was a direct consequence of particle exposure or downstream of inflammation. Nonetheless, our results on the airway smooth muscle cells suggest that direct particle exposure has the potential to effect such smooth muscle inhibition. In another study, nanosized, but not micrometre-sized, carbon black particles were able to inhibit the contraction of collagen matrix by lung fibroblasts; this implies that NPs can impair tissue repair (Kim *et al.* 2003). More importantly, this collagen-gel contraction study also supported the notion that the mechanical function of fibroblasts can be crucial, just as that of skeletal muscle cells, cardiac muscle cells and the airway smooth muscle cells studied here. In this regard, our findings established OMTC as a sensitive, high throughput tool for probing particulate effects on cellular mechanical function.

While previous *in vivo* and *in vitro* studies with inhaled particles had appropriately focused on the inflammatory response in the lung, direct interaction of NPs with key functional cells can potentially result in even more potent functional changes, such as the mechanical ones we demonstrated here. Our results highlight the susceptibility of cellular mechanical function to specific particulate exposure. Future application of cell mechanics to particulate research will help to identify pathogenic particle species or ingredients and contribute to a better understanding of the health effects of particulate exposure on humans.

We thank Douglas Dockery, Justin Mih, Yuan Li, and Dhananjay Tambe for discussions.

REFERENCES

An, S. S., Fabry, B., Trepat, X., Wang, N. & Fredberg, J. J. 2006 Do biophysical properties of the airway smooth muscle in culture predict airway hyperresponsiveness? *Am. J. Respir. Cell Mol. Biol.* **35**, 55–64. (doi:10.1165/rcmb.2005-0453OC)

Antonini, J. M., Lawryk, N. J., Murthy, G. G. & Brain, J. D. 1999 Effect of welding fume solubility on lung macrophage viability and function *in vitro*. *J. Toxicol. Environ. Health A* **58**, 343–363. (doi:10.1080/009841099157205)

Araujo, J. A. *et al.* 2008 Ambient particulate pollutants in the ultrafine range promote early atherosclerosis and systemic oxidative stress. *Circ. Res.* **102**, 589–596. (doi:10.1161/CIRCRESAHA.107.164970)

Bai, T. R. 1990 Abnormalities in airway smooth muscle in fatal asthma. *Am. Rev. Respir. Dis.* **141**, 552–557.

Borm, P. J. & Kreyling, W. 2004 Toxicological hazards of inhaled nanoparticles—potential implications for drug delivery. *J. Nanosci. Nanotechnol.* **4**, 521–531. (doi:10.1166/jnn.2004.081)

Bursac, P., Lenormand, G., Fabry, B., Oliver, M., Weitz, D. A., Viasnoff, V., Butler, J. P. & Fredberg, J. J. 2005 Cytoskeletal remodelling and slow dynamics in the living cell. *Nat. Mater.* **4**, 557–571. (doi:10.1038/nmat1404)

Bursac, P., Fabry, B., Trepat, X., Lenormand, G., Butler, J. P., Wang, N., Fredberg, J. J. & An, S. S. 2007 Cytoskeleton dynamics: fluctuations within the network. *Biochem. Biophys. Res. Commun.* **355**, 324–330. (doi:10.1016/j.bbrc.2007.01.191)

Churg, A., Brauer, M., del Carmen Avila-Casado, M., Fortoul, T. I. & Wright, J. L. 2003 Chronic exposure to high levels of particulate air pollution and small airway remodeling. *Environ. Health Perspect.* **111**, 714–718.

Deng, L., Trepat, X., Butler, J. P., Millet, E., Morgan, K. G., Weitz, D. A. & Fredberg, J. J. 2006 Fast and slow dynamics of the cytoskeleton. *Nat. Mater.* **5**, 636–640. (doi:10.1038/nmat1685)

Deng, X., Luan, Q., Chen, W., Wang, Y., Wu, M., Zhang, H. & Jiao, Z. 2009 Nanosized zinc oxide particles induce neural stem cell apoptosis. *Nanotechnology* **20**, 115 101. (doi:10.1088/0957-4484/20/11/115101)

Dineley, K. E., Votyakova, T. V. & Reynolds, I. J. 2003 Zinc inhibition of cellular energy production: implications for mitochondria and neurodegeneration. *J. Neurochem.* **85**, 563–570.

Dockery, D. W., Luttmann-Gibson, H., Rich, D. Q., Link, M. S., Mittleman, M. A., Gold, D. R., Koutrakis, P., Schwartz, J. D. & Verrier, R. L. 2005 Association of air pollution with increased incidence of ventricular tachyarrhythmias recorded by implanted cardioverter defibrillators. *Environ. Health Perspect.* **113**, 670–674.

Donaldson, K., Tran, L., Jimenez, L. A., Duffin, R., Newby, D. E., Mills, N., MacNee, W. & Stone, V. 2005 Combustion-derived nanoparticles: a review of their toxicology following inhalation exposure. *Part. Fibre Toxicol.* **2**, 10. (doi:10.1186/1743-8977-2-10)

Elson, E. L. 1988 Cellular mechanics as an indicator of cytoskeletal structure and function. *Annu. Rev. Biophys. Chem.* **17**, 397–430. (doi:10.1146/annurev.bb.17.060188.002145)

Fabry, B., Maksym, G. N., Butler, J. P., Glogauer, M., Navajas, D. & Fredberg, J. J. 2001*a* Scaling the microrheology of living cells. *Phys. Rev. Lett.* **87**, 148102. (doi:10.1103/PhysRevLett.87.148102)

Fabry, B., Maksym, G. N., Shore, S. A., Moore, P. E., Panettieri Jr, R. A., Butler, J. P. & Fredberg, J. J. 2001*b* Time course and heterogeneity of contractile responses in cultured human airway smooth muscle cells. *J. Appl. Physiol.* **91**, 986–994.

Fahmy, B. & Cormier, S. A. 2009 Copper oxide nanoparticles induce oxidative stress and cytotoxicity in airway epithelial cells. *Toxicol. In Vitro* **23**, 1365–1371. (doi:10.1016/j.tiv.2009.08.005)

Fredberg, J. J., Jones, K. A., Nathan, M., Raboudi, S., Prakash, Y. S., Shore, S. A., Butler, J. P. & Sieck, G. C. 1996 Friction in airway smooth muscle: mechanism, latch, and implications in asthma. *J. Appl. Physiol.* **81**, 2703–2712.

Frohlich, E., Samberger, C., Kueznik, T., Absenger, M., Roblegg, E., Zimmer, A. & Pieber, T. R. 2009 Cytotoxicity of nanoparticles independent from oxidative stress. *J. Toxicol. Sci.* **34**, 363–375. (doi:10.2131/jts.34.363)

Gazaryan, I. G., Krasinskaya, I. P., Kristal, B. S. & Brown, A. M. 2007 Zinc irreversibly damages major enzymes of energy production and antioxidant defense prior to mitochondrial permeability transition. *J. Biol. Chem.* **282**, 24 373–24 380. (doi:10.1074/jbc.M611376200)

Gehr, P., Bachofen, M. & Weibel, E. R. 1978 The normal human lung: ultrastructure and morphometric estimation of diffusion capacity. *Respir. Physiol.* **32**, 121–140. (doi:10.1016/0034-5687(78)90104-4)

Geiser, M. *et al.* 2005 Ultrafine particles cross cellular membranes by nonphagocytic mechanisms in lungs and in cultured cells. *Environ. Health Perspect.* **113**, 1555–1560.

Helfenstein, M., Miragoli, M., Rohr, S., Muller, L., Wick, P., Mohr, M., Gehr, P. & Rothen-Rutishauser, B. 2008 Effects of combustion-derived ultrafine particles and manufactured nanoparticles on heart cells *in vitro*. *Toxicology* **253**, 70–78. (doi:10.1016/j.tox.2008.08.018)

Henkel, G. & Krebs, B. 2004 Metallothioneins: zinc, cadmium, mercury, and copper thiolates and selenolates mimicking protein active site features—structural aspects and biological implications. *Chem. Rev.* **104**, 801–824. (doi:10.1021/cr020620d)

Karlsson, H. L., Gustafsson, J., Cronholm, P. & Moller, L. 2009 Size-dependent toxicity of metal oxide particles—a comparison between nano- and micrometer size. *Toxicol. Lett.* **188**, 112–118. (doi:10.1016/j.toxlet.2009.03.014)

Kim, H. *et al.* 2003 Ultrafine carbon black particles inhibit human lung fibroblast-mediated collagen gel contraction. *Am. J. Respir. Cell Mol. Biol.* **28**, 111–121. (doi:10.1165/rcmb.4796)

Klein, J. 2007 Probing the interactions of proteins and nanoparticles. *Proc. Natl Acad. Sci. USA* **104**, 2029–2030. (doi:10.1073/pnas.0611610104)

Kreyling, W. G., Semmler, M., Erbe, F., Mayer, P., Takenaka, S., Schulz, H., Oberdorster, G. & Ziesenis, A. 2002 Translocation of ultrafine insoluble iridium particles from lung epithelium to extrapulmonary organs is size dependent but very low. *J. Toxicol. Environ. Health A* **65**, 1513–1530. (doi:10.1080/00984100290071649)

Lehmann, A. D., Blank, F., Baum, O., Gehr, P. & Rothen-Rutishauser, B. M. 2009 Diesel exhaust particles modulate the tight junction protein occludin in lung cells *in vitro*. *Part. Fibre Toxicol.* **6**, 26. (doi:10.1186/1743-8977-6-26)

Li, W. G., Miller Jr, F. J., Brown, M. R., Chatterjee, P., Aylsworth, G. R., Shao, J., Spector, A. A., Oberley, L. W. & Weintraub, N. L. 2000 Enhanced H_2O_2-induced cytotoxicity in 'epithelioid' smooth muscle cells: implications for neointimal regression. *Arterioscler. Thromb. Vasc. Biol.* **20**, 1473–1479.

Li, Y. & Maret, W. 2008 Human metallothionein metallomics. *J. Anal. Atom. Spectrom.* **23**, 1055–1062. (doi:10.1039/b802220h)

Li, Y. & Maret, W. 2009 Transient fluctuations of intracellular zinc ions in cell proliferation. *Exp. Cell Res.* **315**, 2463–2470. (doi:10.1016/j.yexcr.2009.05.016)

Lighty, J. S., Veranth, J. M. & Sarofim, A. F. 2000 Combustion aerosols: factors governing their size and composition and implications to human health. *J. Air Waste Manag. Assoc.* **50**, 1565–1618; discussion 1619–1622.

Lim, C. T., Zhou, E. H., Li, A., Vedula, S. R. K. & Fu, H. X. 2006*a* Experimental techniques for single cell and single molecule biomechanics. *Mater. Sci. Eng. C Biomim. Supramol. Syst.* **26**, 1278–1288.

Lim, C. T., Zhou, E. H. & Quek, S. T. 2006*b* Mechanical models for living cells—a review. *J. Biomech.* **39**, 195–216. (doi:10.1016/j.jbiomech.2004.12.008)

Lin, W., Xu, Y., Huang, C.-C., Ma, Y., Shannon, K., Chen, D.-R. & Huang, Y.-W. 2009 Toxicity of nano- and micro-sized ZnO particles in human lung epithelial cells. *J. Nanopart. Res.* **11**, 25–39. (doi:10.1007/s11051-008-9419-7)

Maret, W. & Li, Y. 2009 Coordination dynamics of zinc in proteins. *Chem. Rev.* **109**, 4682–4707. (doi:10.1021/cr800556u)

Maynard, A. D. *et al.* 2006 Safe handling of nanotechnology. *Nature* **444**, 267–269. (doi:10.1038/444267a)

Mazzola, L. 2003 Commercializing nanotechnology. *Nat. Biotechnol.* **21**, 1137–1143. (doi:10.1038/nbt1003-1137)

Miyoshi, N., Oubrahim, H., Chock, P. B. & Stadtman, E. R. 2006 Age-dependent cell death and the role of ATP in hydrogen peroxide-induced apoptosis and necrosis. *Proc. Natl Acad. Sci. USA* **103**, 1727–1731. (doi:10.1073/pnas.0510346103)

Muhlfeld, C., Geiser, M., Kapp, N., Gehr, P. & Rothen-Rutishauser, B. 2007 Re-evaluation of pulmonary titanium dioxide nanoparticle distribution using the 'relative deposition index': evidence for clearance through microvasculature. *Part. Fibre Toxicol.* **4**, 7. (doi:10.1186/1743-8977-4-7)

Müller, L., Riediker, M., Wick, P., Mohr, M., Gehr, P. & Rothen-Rutishauser, B. 2009 Oxidative stress and inflammation response after nanoparticle exposure: differences between human lung cell monocultures and an advanced three-dimensional model of the human epithelial airways. *J. R. Soc. Interface* **7**(Suppl. 1), S27–S40. (doi:10.1098/rsif.2009.0161.focus)

Nel, A., Xia, T., Madler, L. & Li, N. 2006 Toxic potential of materials at the nanolevel. *Science* **311**, 622–627. (doi:10.1126/science.1114397)

Nicod, L. P. 2005 Lung defences: an overview. *Eur. Respir. Rev.* **14**, 45–50. (doi:10.1183/09059180.05.00009501)

Oberdorster, G., Oberdorster, E. & Oberdorster, J. 2005 Nanotoxicology: an emerging discipline evolving from studies of ultrafine particles. *Environ. Health Perspect.* **113**, 823–839.

Pandya, H. C., Snetkov, V. A., Twort, C. H., Ward, J. P. & Hirst, S. J. 2002 Oxygen regulates mitogen-stimulated proliferation of fetal human airway smooth muscle cells. *Am. J. Physiol. Lung Cell Mol. Physiol.* **283**, L1220–L1230.

Paull, R., Wolfe, J., Hebert, P. & Sinkula, M. 2003 Investing in nanotechnology. *Nat. Biotechnol.* **21**, 1144–1147. (doi:10.1038/nbt1003-1144)

Penttinen, P., Timonen, K. L., Tiittanen, P., Mirme, A., Ruuskanen, J. & Pekkanen, J. 2001 Ultrafine particles in urban air and respiratory health among adult asthmatics. *Eur. Respir. J.* **17**, 428–435. (doi:10.1183/09031936.01.17304280)

Peters, A., Wichmann, H. E., Tuch, T., Heinrich, J. & Heyder, J. 1997 Respiratory effects are associated with the number of ultrafine particles. *Am. J. Respir. Crit. Care Med.* **155**, 1376–1383.

Peters, A., Dockery, D. W., Muller, J. E. & Mittleman, M. A. 2001 Increased particulate air pollution and the triggering of myocardial infarction. *Circulation* **103**, 2810–2815.

Pinkerton, K. E. *et al.* 2000 Distribution of particulate matter and tissue remodeling in the human lung. *Environ. Health Perspect.* **108**, 1063–1069. (doi:10.2307/3434960)

Pisanic II, T. R., Blackwell, J. D., Shubayev, V. I., Finones, R. R. & Jin, S. 2007 Nanotoxicity of iron oxide nanoparticle internalization in growing neurons. *Biomaterials* **28**, 2572–2581. (doi:10.1016/j.biomaterials.2007.01.043)

Pope, C. A., Dockery, D. W. & Schwartz, J. 1995 Review of epidemiological evidence of health effects of particulate air pollution. *Inhal. Toxicol.* **7**, 1–18. (doi:10.3109/08958379509014267)

Pope III, C. A., Ezzati, M. & Dockery, D. W. 2009 Fine-particulate air pollution and life expectancy in the United States. *N. Engl. J. Med.* **360**, 376–386. (doi:10.1056/NEJMsa0805646)

Rothen-Rutishauser, B. M., Kiama, S. G. & Gehr, P. 2005 A three-dimensional cellular model of the human respiratory tract to study the interaction with particles. *Am. J. Respir. Cell Mol. Biol.* **32**, 281–289. (doi:10.1165/rcmb.2004-0187OC)

Rothen-Rutishauser, B., Muhlfeld, C., Blank, F., Musso, C. & Gehr, P. 2007 Translocation of particles and inflammatory responses after exposure to fine particles and nanoparticles in an epithelial airway model. *Part. Fibre Toxicol.* **4**, 9. (doi:10.1186/1743-8977-4-9)

Rothen-Rutishauser, B., Blank, F., Muhlfeld, C. & Gehr, P. 2008 *In vitro* models of the human epithelial airway barrier to study the toxic potential of particulate matter. *Expert Opin. Drug Metab. Toxicol.* **4**, 1075–1089. (doi:10.1517/17425255.4.8.1075)

Rothen-Rutishauser, B., Blank, F., Mühlfeld, C. H. & Gehr, P. 2009 Nanoparticle–cell membrane interactions. In *Particle–lung interactions* (eds P. Gehr, F. Blank, C. H. Mühlfeld & B. Rothen-Rutishauser), 2nd edn. New York, NY: Informa Healthcare.

Sager, T. M. & Castranova, V. 2009 Surface area of particle administered versus mass in determining the pulmonary toxicity of ultrafine and fine carbon black: comparison to ultrafine titanium dioxide. *Part. Fibre Toxicol.* **6**, 15. (doi:10.1186/1743-8977-6-15)

Sager, T. M., Kommineni, C. & Castranova, V. 2008 Pulmonary response to intratracheal instillation of ultrafine versus fine titanium dioxide: role of particle surface area. *Part. Fibre Toxicol.* **5**, 17. (doi:10.1186/1743-8977-5-17)

Schulz, H. *et al.* 2005 Cardiovascular effects of fine and ultrafine particles. *J. Aerosol Med.* **18**, 1–22. (doi:10.1089/jam.2005.18.1)

Sharpley, M. S. & Hirst, J. 2006 The inhibition of mitochondrial complex I (NADH : ubiquinone oxidoreductase) by Zn^{2+}. *J. Biol. Chem.* **281**, 34 803–34 809. (doi:10.1074/jbc.M607389200)

Shore, S. A. 2004 Airway smooth muscle in asthma—not just more of the same. *N. Engl. J. Med.* **351**, 531–532. (doi:10.1056/NEJMp048139)

Suresh, S. 2007 Biomechanics and biophysics of cancer cells. *Acta Biomater.* **3**, 413–438. (doi:10.1016/j.actbio.2007.04.002)

Trepat, X., Deng, L., An, S., Navajas, D., Tschumperlin, D., Gerthoffer, W., Butler, J. & Fredberg, J. 2007 Universal physical responses to stretch in the living cell. *Nature* **447**, 592–595. (doi:10.1038/nature05824)

Waters, K. M. *et al.* 2009 Macrophage responses to silica nanoparticles are highly conserved across particle sizes. *Toxicol. Sci.* **107**, 553–569. (doi:10.1093/toxsci/kfn250)

Weichenthal, S., Dufresne, A. & Infante-Rivard, C. 2007 Indoor ultrafine particles and childhood asthma: exploring a potential public health concern. *Indoor Air* **17**, 81–91. (doi:10.1111/j.1600-0668.2006.00446.x)

Wichmann, H. E., Spix, C., Tuch, T., Wolke, G., Peters, A., Heinrich, J., Kreyling, W. G. & Heyder, J. 2000 Daily mortality and fine and ultrafine particles in Erfurt, Germany part I: role of particle number and particle mass. *Res. Rep. Health Eff. Inst.* **98**, 5–86, discussion 87–94.

Xia, T. *et al.* 2006 Comparison of the abilities of ambient and manufactured nanoparticles to induce cellular toxicity according to an oxidative stress paradigm. *Nano Lett.* **6**, 1794–1807. (doi:10.1021/nl061025k)

Xia, T., Kovochich, M., Liong, M., Madler, L., Gilbert, B., Shi, H., Yeh, J. I., Zink, J. I. & Nel, A. E. 2008 Comparison of the mechanism of toxicity of zinc oxide and cerium oxide nanoparticles based on dissolution and oxidative stress properties. *ACS Nano* **2**, 2121–2134. (doi:10.1021/nn800511k)

Yu, L. E., Lanry Yung, L.-Y., Ong, C.-N., Tan, Y.-L., Suresh Balasubramaniam, K., Hartono, D., Shui, G., Wenk, M. R. & Ong, W.-Y. 2007 Translocation and effects of gold nanoparticles after inhalation exposure in rats. *Nanotoxicology* **1**, 235–242. (doi:10.1080/17435390701763108)

Zhou, E. H. *et al.* 2009 Universal behavior of the osmotically compressed cell and its analogy to the colloidal glass transition. *Proc. Natl Acad. Sci. USA* **106**, 10 632–10 637. (doi:10.1073/pnas.0901462106)

Zhou, E. H., Quek, S. T. & Lim, C. T. In press. Power-law rheology analysis of cells undergoing micropipette aspiration. *Biomech. Model. Mechanobiol.* (doi:10.1007/s10237-010-0197-7)

Zhu, C., Bao, G. & Wang, N. 2000 Cell mechanics: mechanical response, cell adhesion, and molecular deformation. *Ann. Rev. Biomed. Eng.* **2**, 189–226. (doi:10.1146/annurev.bioeng.2.1.189)